DOI: https://doi.org/10.37434/tpwj2024.05.07

SIMULATION OF ELECTRIC ARC MODE OF ELECTRIC FURNACE AND ANALYSIS OF ITS OPERATION IN REAL TIME

M.M. Gasik

Aalto University, 00076, AALTO, Espoo, Finland

ABSTRACT

A model of a three-phase electric furnace is considered, for which the distribution of temperature and electric field over the volume is calculated. Areas of the furnace are shown, in which extreme values of current density and temperature occur. The simulation results are compared with the real data of the 12 MVA furnace operation in factory conditions, and the features of the furnace operation in various modes are discussed.

KEYWORDS: simulation, furnace, electric mode, temperature distribution, current density

INTRODUCTION

Ore-renovation electric furnaces in the production of ferroalloys, mattes, molten refractories, slag and other products at high temperatures use high-power current, operating in arc, arc-free or mixed electric modes [1, 2]. Arc-free mode is typical of multislag processes, where reactions occur on the slag-melt interface, and the electric arc is almost absent. An example of such a process may be manganese slag dephosphorization for melting silicomanganese, higher grades of ferromanganese and metal manganese [2] and processes of slag refining in the production of copper, nickel and metals of the platinum group [3].

Despite the absence of an electric arc in the working volume and the associated turbulence of melts movement, the analysis of such thermal and electric modes of furnaces is a complex problem as far as it has many uncertain parameters and their direct experimental measurement is often impossible. Thus, simulation of the furnace operation allows evaluating and predicting local values of important variables (temperature, current density, speed of movement of metal and slag flows, kinetics of chemical reactions, etc.), if the corresponding parameters were applied during simulation. The best result can be obtained during experimental confirmation of the model in real time, but in factory conditions, the amount of data being registered is rather limited. Earlier, the authors have shown that such models can be used with high efficiency when analyzing the operation of electrocalcinators for thermoanthracite production [4], where it is impossible to obtain direct data directly from the volume of the calcinator.

For the purpose of developing a well-grounded and adjusted model, in this research, the 12 MVA furnace in the arc-free mode, its electrical and thermal parameters, measured in the real-time mode and the appropriate digital twin for calculations are considered.

FURNACE MODEL AND RESULTS OF CALCULATIONS

The model of a three-phase electric furnace, operating in the resistance mode (arc-free mode) with a diameter of 13 m, with self-sintering electrodes of 1100 mm diameter and a rated capacity of 12 MVA was created with the COMSOL Multiphysics 5.4 package. The model includes furnace casing with lining, closed flue, molten metal and slag volumes and upper interlayer rich in coke (Figure 1). All materials have set equations of heat and electrical conductivity, heat capacity, density, etc. depending on the temperature, and for the liquid phase, the viscosity equation is also added [5]. Thermal mode of the furnace in the model is introduced by general differential equations of heat conductivity and convective heat exchange, and electric mode is introduced by the system of Ampere–Maxwell's equations, where the vector of current density **J**:

$$\mathbf{J} = \nabla\times\mathbf{H} = \sigma(\mathbf{E} + \mathbf{v}\times\mathbf{B}) + i\omega\mathbf{D} + \mathbf{J}_{ext}, \quad (1)$$

where **H** is the vector of magnetic field elasticity; **E** is the vector of electric field strength; **v** is the speed of movement of electrically conductive environment; **B** is the vector of magnetic induction; **D** is the vector of electric displacement; $i = \sqrt{-1}$, $\omega = 2\pi f$ is the angular frequency of the field ($f = 50$ Hz); $\mathbf{J}_{ext}$ is the density of external current (in the case is absent); σ is the electrical conductivity of the environment. Differential equations based on the electric field intensity $\mathbf{E} = -\nabla\varphi$ have the following form:

Copyright © The Author(s)

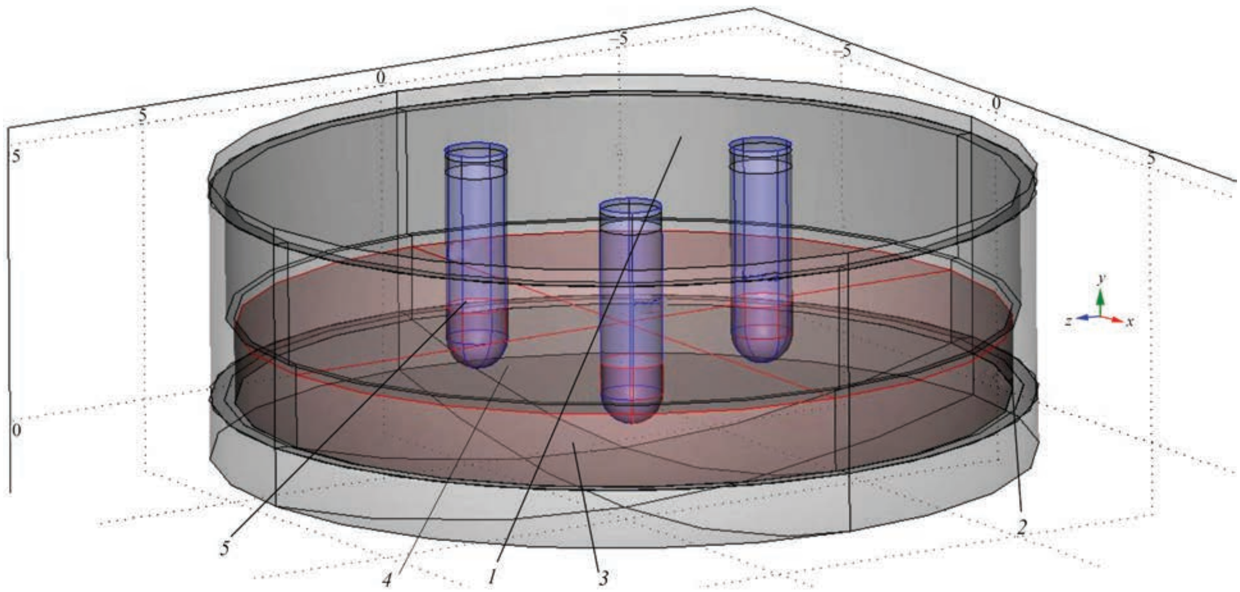

Figure 1. Scheme of three-phase furnace model (coordinate sizes in meters): *1* — crypt; *2* — wall; *3* — bottom-plate; *4* — melt; *5* — electrode

$$\begin{gathered}-\nabla\left(\left(i\omega\sigma-\omega^2\varepsilon\varepsilon_0\right)\mathbf{A}-\sigma\mathbf{v}\left(\nabla\times\mathbf{A}\right)+\right.\\ \left.+\left(\sigma+i\omega\varepsilon\varepsilon_0\right)\nabla\phi-\left(\mathbf{J}_{ext}+i\omega\mathbf{P}\right)\right)=0;\\ \left(i\omega\sigma-\omega^2\varepsilon\varepsilon_0\right)\mathbf{A}+\nabla\left(\left(\mu\mu_0\right)^{-1}\nabla\times\mathbf{A}-\mathbf{M}\right)-\\ -\sigma\mathbf{v}\left(\nabla\times\mathbf{A}\right)+\left(\sigma+i\omega\varepsilon\varepsilon_0\right)\nabla\phi=\mathbf{J}_{ext}+i\omega\mathbf{P},\end{gathered} \tag{2}$$

where **A** is the vector magnetic potential; φ is the scalar electric potential; **M** is the vector of magnetization environment; μ is the relative magnetic permeability; $\mu_0 = 4\pi\cdot10^{-7}$ is the magnetic permeability of vacuum. It should be emphasized that the calculations consider the entire volume of the furnace with electrodes, lining and casing. Therefore, in equations (*1*, *2*), a magnetic contribution for metal design elements can be very significant. These equations do not have a clear temperature contribution, but almost all variables depend on the temperature. Thermal model of the furnace has a contribution from the electric W_e and magnetic W_m powers of the system:

$$\begin{gathered}W_e=\int_\Omega\left(\int_0^T\mathbf{E}\frac{\partial\mathbf{D}}{\partial t}dt\right)d\Omega;\\ W_m=\int_\Omega\left(\int_0^T\mathbf{H}\frac{\partial\mathbf{B}}{\partial t}dt\right)d\Omega,\end{gathered} \tag{3}$$

where Ω is the volume of the furnace (with electrodes and lining): $T = 1/f$ is the period of current harmonics (1/50 s). Partial derivatives from W_e and W_m in time are electric and magnetic powers, respectively, the sum of which is associated with ohmic (active) and reactive components of the Poynting theorem:

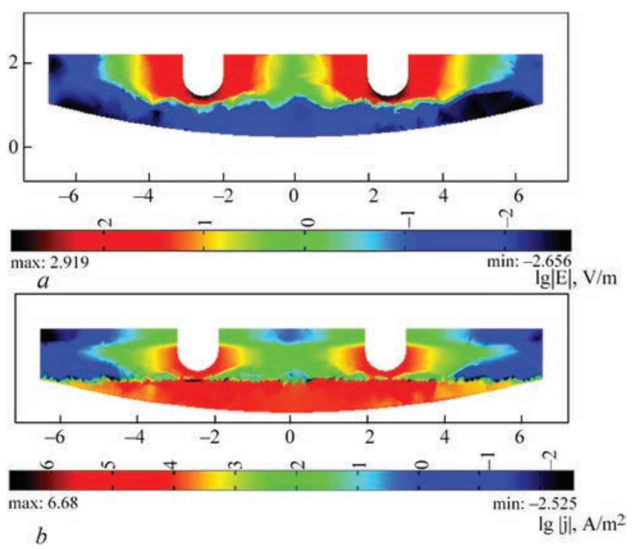

Figure 2. Logarithms of amplitude of electric field gradient (*a*) and current density in the furnace cross-section (*b*). Digits of colour scale — logarithms relative to electric field gradient (V/m) and current density (A/m²)

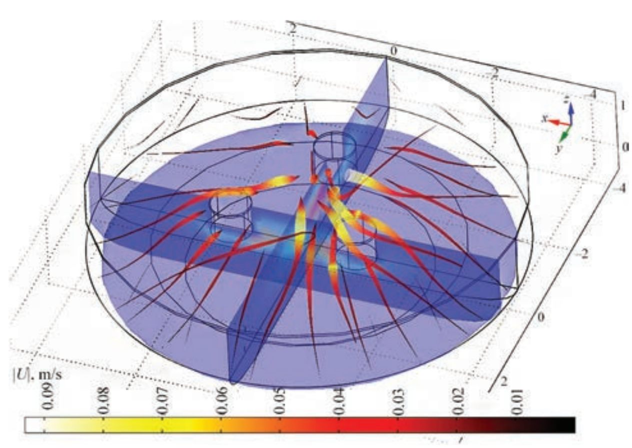

Figure 3. Amplitude of melt movement speed in a three-phase furnace model

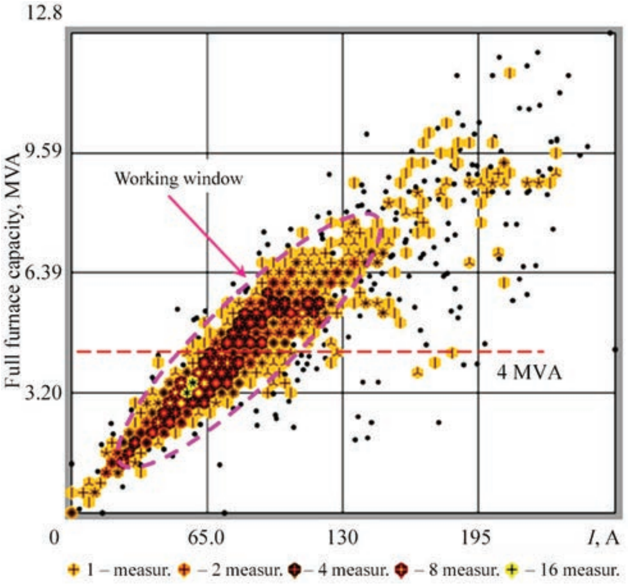

Figure 4. Power as a transformer primary current function (log data on real-time furnace operation[*])

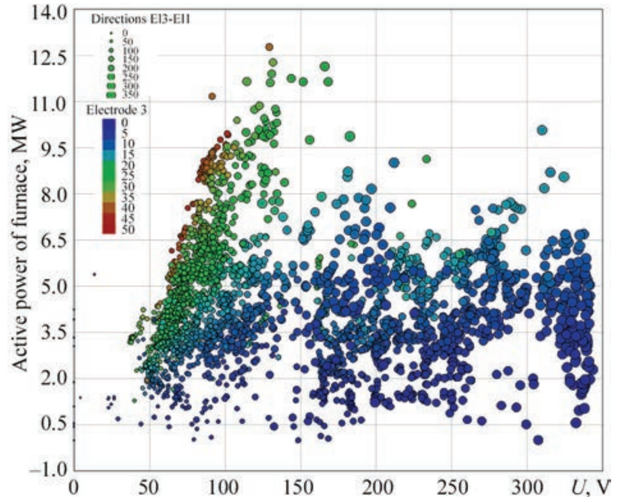

Figure 6. Active power as a voltage function between the third electrode and hearth of the furnace (log data on real-time furnace operation are presented in a 4D-format)

$$-\int_\Omega\left(\mathbf{E}\frac{\partial \mathbf{D}}{\partial t}+\mathbf{H}\frac{\partial \mathbf{B}}{\partial t}\right)d\Omega = \int_\Omega \mathbf{J}\cdot\mathbf{E}\,d\Omega + \oint_S \left(E\times H\right)\mathbf{n}\,dS, \qquad (4)$$

where **n** is the normal vector to the surface S, limiting the volume Ω of the furnace. The first member in the right part of the equation (4) is the ohmic losses (Joule heat) and the second one is the reactive and radiation electromagnetic losses. Ohmic losses are added to the heat transfer equations as a generated thermal power together with the enthalpy of chemical reactions. Thus, the system of basic differential equations is nonlinear and it requires iterative solutions together with the heat and mass exchange equations [4, 5].

On the electrodes in the model of this research, a harmonic phase voltage with an amplitude of 140 V and a frequency of 50 Hz was applied, and these pa-

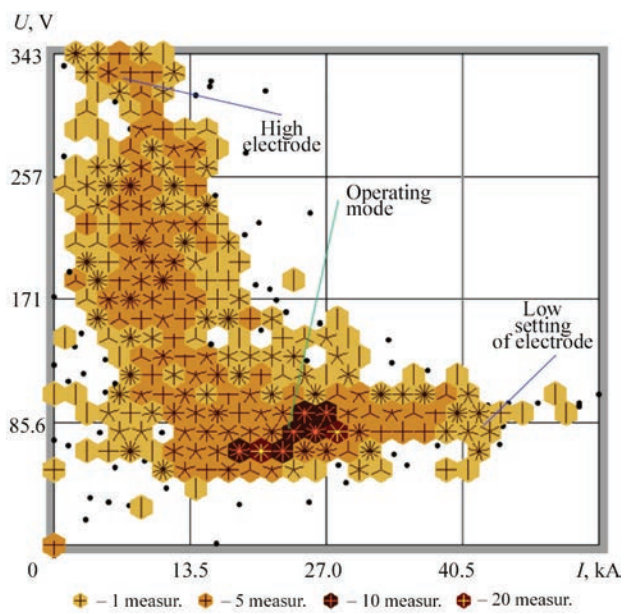

Figure 5. Voltage between the first electrode and hearth of the furnace and current on the first electrode (log data on real-time furnace operation)

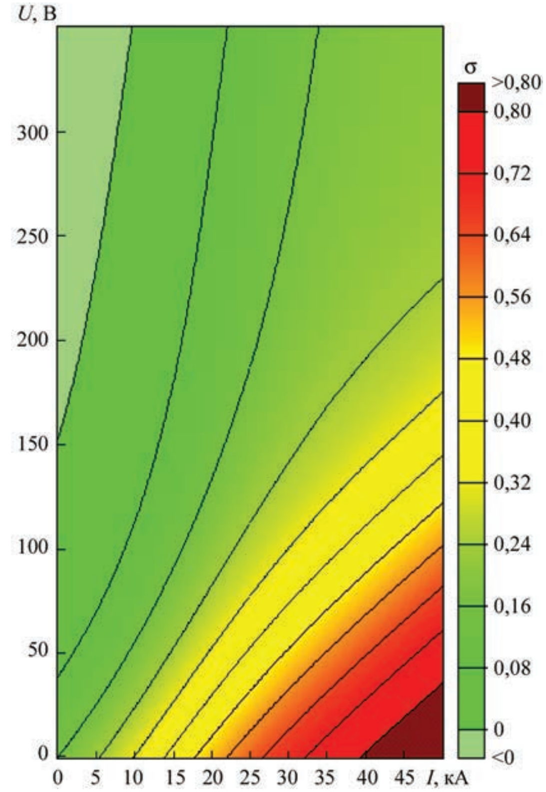

Figure 7. Dependence of effective electrical conductivity on voltage between the electrodes and electrode current according to the results of neural network computations [6]

[*]The average value of the furnace power in the analyzed month was about 4 MVA (red line). The oval outlines the range of primary current of the transformer and the furnace power, in which the furnace operated the longest amount of time.

rameters were used to calculate the distributions of electric field gradient |**E**| in the volume (Figure 2, *a*) and current density (Figure 2, *b*). According to the results (Figure 2), the highest current density is observed near the ends of the electrodes between the electrodes and inside the molten metal (>10^6 A/m^2), whereas near the lining of the furnace, it is reduced to 0.003 A/m^2.

Since the specific electrical resistance of the metal is much lower than that in slag or coke interlayer, active power and, accordingly, thermal power also exhibit low values there. Thus, the highest thermal power is observed directly in the area of the electrodes immersed in slag (in Figure 2, exactly in the locations of the reddest zones for the electric field and current density at the same time).

The uneven distribution of power and temperature leads to the convection movement of metal and slag melts, the maximum of which (up to 0.1 m/s) is observed near the electrodes as a result of lower viscosity and higher temperature gradients in these areas (Figure 3).

ANALYSIS OF REAL FURNACE OPERATION

For the electric furnace similar to the model above, experimental data (approximately 4,000 lines of temperature and electrical logs data collected in a one calendar month) were collected in real factory conditions. The furnace with a rated capacity of 12 MVA is operating to refine slag in a limited temperature range and, therefore, it usually operates with much lower electrical load compared to its rated capacity. The ellipse dotted line (Figure 4) outlines the working window of the electric furnace mode (the highest statistical amount of data), but there are also more distant points for various reasons (electrodes freezing, short circuit, incorrect movement or electrode breakdown, other reasons, maintenance, etc.).

An unconventional format of the diagram (Figure 4) allows covering the whole picture of the furnace operation. For example, a yellow point with six “petals” indicates here 96 (16×6) measurements, since one petal is equal to 16 measurements, having the same value. For a dark yellow point, one petal is equal to one measurement, for black one — four measurements, etc. This allows showing high dimensionality data in a 2D-diagram. Figure 5 shows data on voltage between the first electrode and hearth of the furnace and current on the first electrode. These data indicate in particular the frequency of furnace staying with a high or low electrode, as well as the area of the highest number of cases of normal operation (for example at 70–120 V and 20–30 kA).

Data of the furnace operation can also be represented in a 4D format (Figure 6), where along the abscissa axis, voltage between the third electrode and hearth of the furnace is marked; along the ordinate axis, active power is marked and the colour of each point corresponds to the value of current on the electrode at a moment and the size of a point corresponds to the voltage between the first and third electrodes.

Results in Figure 6 indicate essential features in the furnace operation. Thus, red points (high current of up to 50 kA) show the limit of power and voltage, which are regulated by the overall electrical resistance of the furnace at a particular measurement moment. Large blue points indicate a high electrode setting (low current and high voltage), and small blue points indicate cases of rising and switching off electrodes (low active power at low current and voltage).

The electrical power system of the furnace is based on transformers converting input high mains voltage and low current on the primary side to a level suitable for the furnace operation [1]. At normal operation, all three transformers have the same parameters that provide symmetrical conditions of the furnace operation. If displaced settings occur (points in Figures 4–6, that deviate significantly from the working area), this leads to circulating unbalanced currents in triangular connections [5], which may be not detected by standard measurements, that may cause malfunction of the electrical equipment (except for the cases of normal technological maintenance).

From Figures 4 and 5, it is seen how the change in the electrode position affects the flow direction of current and power. In turn, the area near the ends of the electrodes (Figure 2) is hotter and has a lower resistance. Therefore, it is necessary to avoid direct immersion into the molten metal as it will lead to electric breaking.

The results show that even simple electrotechnical log data contain a considerable amount of information, which at the moment of required visualization can indicate many significant parameters regarding deviations from optimal modes and possible ways to improve operation of the furnace. It is also necessary to point out the agreement of the model values with real data, which makes it possible to create the so-called digital twin of the furnace and simulate its operation in computer networks. Figure 7 shows the calculated efficient electrical conductivity depending on the voltage between the electrodes and the electrode current, which was generated by a neural network computation on the example of [6] based on the real furnace data given above (Figures 4–6) and the proposed computer model (Figures 1–3).

Results in Figure 7 show that at a low electrode position (high current, low voltage gradient), the efficient electrical conductivity (taking into account the metal, slag and coke interlayer) is the highest and it is significantly non-linear in relation to electrical parameters of the furnace. Such tools can be used to simulate different situations of the furnace to determine its optimal operation.

CONCLUSIONS

1. The model of the ore-renovation 12 MVA furnace was designed and shown, for which the distributions of electric field gradient in the volume, current density and movement of molten metal and slag as a result of temperature gradient and melt properties were calculated.

2. In parallel with the simulation, log data of the furnace operation in factory conditions in real-time modes were analyzed and options for visual analysis of this data were presented, which helps to understand the furnace operation and the reasons for deviation of the electric mode from the set one.

3. By combination of the model and real data, the possibility of creating digital twin of the furnace was shown, where parameters can be calculated and different furnace situations can be simulated to determine the optimal operation.

4. The carried out analysis shows the possibilities of using modern computing tools to control the operation of metallurgical units and their further improvement.

REFERENCES

1. Gladkykh, V.A., Gasyk, M.I., Ovcharuk, A.M., Projdak, Yu.S. (2004) *Design and equipment of electric steel making and ferroalloy shops.* Dnipropetrovsk, Systemni Tekhnologii [in Ukrainian].
2. Gasik, M.I. (1992) Manganese. Moscow, Metallurgiya [in Russian].
3. Larsen, B. (2012) Electrode models for Søderberg electrodes. In: *Proc. SAIMM «Platinum 2012», South Africa, Johannesburg*, 275–286.
4. Gasik, M.M., Gasik, M.I., Urazlina, O.Yu., Kutuzov, S.V. (2010) Modelling and optimisation of anthracite treatment in an electrocalcinator. In: *Proc. of 12th Inter. Ferroalloys Congr. INFACON, Helsinki, Finland*, **1**, 339–347.
5. Gasik, M. (2013) *Handbook of Ferroalloys: Theory and Technology*. Elsevier/Butterworth-Heinemann, Oxford, UK.
6. Gasik, M.M., Gasik, M.I. (2010) Multi-variation analysis and optimisation of electrical conductivity of MnO–CaO–SiO_2 slags. In: *Proc. of 12th Inter. Ferroalloys Congr. INFACON, Helsinki, Finland*, **2**, 537–545.

ORCID

M.M. Gasik: 0000-0002-5782-7987

CORRESPONDING AUTHOR

M.M. Gasik

Aalto University, 00076, AALTO, Espoo, Finland.

E-mail: michael.gasik@aalto.fi

SUGGESTED CITATION

M.M. Gasik (2024) Simulation of electric arc mode of electric furnace and analysis of its operation in real time. *The Paton Welding J.*, **5**, 48–52.

JOURNAL HOME PAGE

https://patonpublishinghouse.com/eng/journals/tpwj

Received: 18.02.2024
Received in revised form: 25.03.2024
Accepted: 07.06.2024